A SIGNAL PROCESSING SCHEME FOR A MULTICHANNEL PASSIVE RADAR SYSTEM

James Palmer

Defence Science and Technology Organisation, Australia

ABSTRACT

In this paper we describe a processing scheme for direction of arrival estimation using multichannel data in a broadcast digital television based passive radar system. We discuss the interrelationship between the clutter cancellation stage and the performance of the direction of arrival (DoA) estimation stage and show that imperfect knowledge of the reference signal leads to a non-uniform noise energy distribution in the spatial dimensions in the processing scheme employed.

Index Terms— Passive Radar, Passive Bistatic Radar, Direction Finding, Clutter Cancellation

1. INTRODUCTION

Passive radar is a reemerging technology area that has received much attention in the academic and defence sectors in the past decade [1, 2, 3, 4, 5, 6]. Whilst passive radar has a number of strengths and weaknesses with respect to cooperative and active monostatic radar, it is the author's opinion that the recent resurgence in interest is primarily due to three dominant factors: 1) Spectrum congestion and diminishing allocation for active radar has motivated the search for viable alternatives; 2) Improvements in technology have overcome some historical limitations (computational complexity and synchronisation issues to name two); and 3) the transmitters typically considered most suitable from an exploitation standpoint (namely broadcast television and radio) have seen a change in their modulation structures from analogue to digital; this has greatly simplified the necessary processing, and improved system performance, reliability and resolution.

Passive radars that exploit broadcast signals are unique in the field of radar systems for several reasons:

Firstly, in the typical application, there is an inherent asymmetry between the transmitter and receiver in terms of their beampatterns and coverage regions that doesn't exist in monostatic radar. As such, and given the potentially omnidirectional nature of the transmitter, it makes sense for the receiver to be similarly able to search all directions of interest[1] simultaneously. This field-of-view requirement leads to the need for multichannel implementations that possess the ability to simultaneously search wide (potentially hemispherical) fields-of-regard with as much sensitivity (i.e. effective collection area) practicable. In this paper, we consider the case of a ring array of omni-directional folded dipole elements to attempt to meet this need. A search of the passive radar literature indicates that this solution appears as a common convergence; a fact that is likely due to the reasoning stated above [7, 8, 9, 10].

Secondly, and in a related direction, most passive radar systems operate by exploiting a source of continuous wave (CW) illumination. This may be both a blessing and a curse, as the radar must operate in an environment with high levels of continuous interference from the source and clutter environment yet the radar is less bound by a transmitter driven time schedule for any search direction. This means the passive radar can achieve a high update rate with low complexity RF hardware (i.e. there is no need to support non-linear beam steering required for pulse chasing). Taken together with the antenna asymmetry, this creates an opportunity for hemispherical, persistent surveillance.

Lastly, in traditional radar systems complete knowledge of the transmitted waveform may be assumed. This is not so in the case of passive radar where knowledge of the transmitter's waveform is most typically obtained via direct signal measurement and, as such, is inherently imperfect.

In this paper, we will investigate a computationally tractable processing scheme that permits hemispherical, persistent surveillance and furthermore demonstrate the effect that imperfect knowledge of the transmitted waveform can have on system performance.

2. SIGNAL MODEL

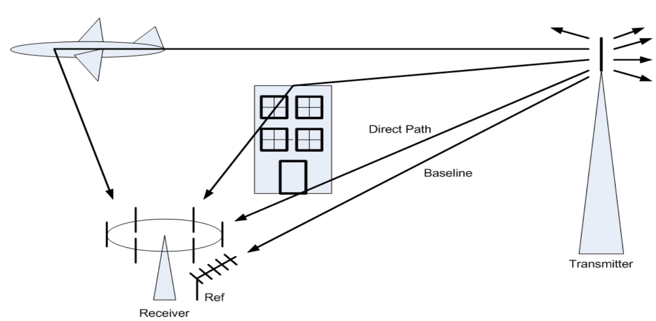

Fig. 1. System geometry

[1] which in many cases may be 360° in azimuth

In developing the signal model for this paper, we assume the system geometry depicted in Figure 1; which consists of a static transmitter and receiver. In this case, we have an N channel surveillance antenna (represented by $\boldsymbol{s_n}$), as well as a reference channel ($\boldsymbol{r}$). $\boldsymbol{r}$ may come from either a dedicated reference antenna (as shown in Figure 1), or it may result from specifically beamformed surveillance channels. The originally transmitted signal is $\boldsymbol{x}$. $\boldsymbol{r}$ may be modelled as:

$$\boldsymbol{r} = \alpha \boldsymbol{x} + X_K \boldsymbol{\gamma} + \boldsymbol{\eta_r} \tag{1}$$

where α is a complex scalar that accounts for propagation effects, X_K is the $(N_{CPI} \times K)$ reference signal matrix that has time delayed versions of $\boldsymbol{x}$ as its columns, and $\boldsymbol{\eta_r}$ is the sensor noise and other imperfections. $\boldsymbol{s_n}$ is:

$$\boldsymbol{s_n} = X_C \boldsymbol{\omega} + \boldsymbol{\eta_{s,n}} \tag{2}$$

where $\boldsymbol{\omega}$ is the $(C \times 1)$ weight vector for the direct path interference (DPI) and static clutter, X_C is the $(N_{CPI} \times C)$ reference signal matrix. The 1st column of this matrix is the signal vector $\boldsymbol{x}$ subsequent columns are time delayed versions of the reference signal. $\boldsymbol{\eta_{s,n}}$ incorporates the sensor noise and any moving targets of interest.

3. PROCESSING SCHEME

The processing scheme developed in this paper is motivated by several requirements: 1) It must achieve high accuracy delay, Doppler and direction of arrival (DoA) estimates; 2) It must maximise target SNR in order to improve probability of detection; and 3) It must minimise computational overhead (both in terms of processing and data volume sizes required for distribution) such that real-time implementations may be feasible on modest hardware. Unfortunately, the third motivating requirement typically acts to counteract the first two. As such, a suitable trade-off between the three is sought.

3.1. Scenario

In order to permit an indicative analysis of alternate approaches, we introduce a representative system. Table 1 shows that we are considering a six element ring array with a dedicated reference antenna for LOS signal collection (i.e. seven channels in all). For our DoA analysis, we are considering a total of 1440 {azimuth, elevation} hypotheses.

Figure 2 shows the "far-field" cartesian hypotheses that correspond to the DoA hypotheses that we desire to test to determine the presence or absence of one or more targets. These points are used to generate the 6×1 steering vectors to be used in conjunction with the surveillance array data. The surveillance array is visible as a red dot in the middle of the x-y plane in Figure 2.Using the geometry shown in Figure 2, we are able to calculate the set of steering vectors by using the equation:

$$a_{h,n} = e^{-j\phi_{h,n}} \tag{3}$$

Table 1. System parameters

Description	Value
Surveillance Elements (N)	6
Reference Elements	1
DOA Hypotheses (Az × El)	360×4
Surveillance array configuration	Ring
Surveillance element type	Dipole
Coherent Processing Interval (CPI)	0.1 s
IQ Sample Rate	8 MSps

where $\phi_{h,n} = \frac{2\pi R_{h,n}}{\lambda}$,
$R_{h,n} = \sqrt{(x_h - x_n)^2 + (y_h - y_n)^2 + (z_h - z_n)^2}$, and (x_n, y_n, z_n) and (x_h, y_h, z_h) are the cartesian coordinates of the element and the hypothesis under test, respectively.

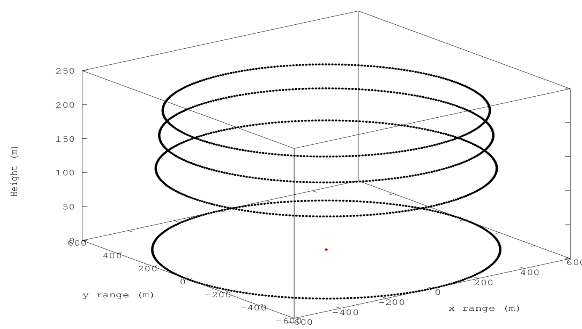

Fig. 2. Steering Vector Hypotheses

3.2. Approach

In contextualising our approach, we consider a relatively standard methodology in terms of signal processing stages; i.e. we will assume the need for a direction finding / beamforming stage, a clutter mitigation stage, and a delay-Doppler map formation stage[2]. Whilst we have identified the need for these stages, we have not yet identified the implementation details for each stage, nor the order of processing; these factors shall be influenced by the requirements stated in Section 3.

It is apparent from the literature [11, 12, 2, 6], that cross-ambiguity processing of noise-like CW signals with moderate bandwidths provides adequate to high quality target parameter estimation, resulting in good target separation. Signals often used in passive radar, such as Digital Video Broadcast - Terrestrial (DVB-T) and Digital Audio Broadcast (DAB) signals, belong to this class of signal. It is also readily apparent that, as these signals are typically in the VHF / UHF region, achieving high accuracy direction of arrival estima-

[2]Detection and tracking stages would also typically be required but they will not be considered here due to space constraints.

tion through the use of highly directive, and therefore sufficiently large, antennas is impractical. Figure 3 shows the directional response that is achievable using a six element ring array with a $\lambda/2$ element spacing. As shown, this beampattern has a coarse level of angular discrimination ($\sim 50°$ at the half power points) and sidelobe levels that would result in difficulties discerning between widely spaced targets were their signal strengths widely varying. Given these two observations, it appears that target discrimination/separation appears to be more achievable in the delay-Doppler domain than in the angular domain.

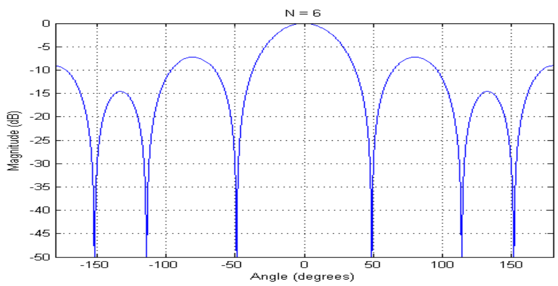

Fig. 3. Simulated Array response

3.2.1. *Computational Considerations*

Given the number of DoA hypotheses in a typical scenario (c.f. Table 1), digitally forming a beam in the time domain for each hypothesis (shown in Figure 2) would require a moderate amount of computation and generate a significant volume of data (in our scenario this would be 1440 time series with N_{CPI} samples in each per CPI). Even if we only applied the minimal subsequent step of delay-Doppler map formation[3] for each beam's time series, real-time tractability appears unlikely (i.e. need to form 1440 beams and delay-Doppler maps in less time than it takes to collect a CPI's worth of data).

By forming delay-Doppler maps on each element, we constrain the number of delay-Doppler maps required to N channels (six in our scenario), which greatly reduces both the data volume and computational requirement. If we permit one moderate simplifying assumption, a further improvement can be achieved. This assumption is: in any given delay-Doppler bin only one target may be present (i.e. a zero or one target hypothesis). Given the delay and Doppler resolution of the system, the validity of this assumption is quite likely. Under this assumption, we are able to calculate all directional hypotheses post delay-Doppler map (post-dDM - i.e. using N samples from each delay-Doppler point independently), but we only need to retain the peak value and its location, instead of this information for the entire azimuth and elevation test space. As such, at the output of the direction finding stage, we are left with a 3D matrix of dimensions: $(N_\tau \times N_\nu \times 3)$, where N_τ and N_ν are the number of delay points and Doppler points under consideration, respectively, and the layers of the third dimension represent the peak signal value, azimuth and elevation of arrival, respectively. Compared with the input data volume of $(N_\tau \times N_\nu \times N)$ $(N = 6$ in our case) or with the pre-delay-Doppler digital beamforming approach discussed earlier ($(N_\tau \times N_\nu \times (360 \times 4))$ for comparable angular sensitivity), we realise a modest to significant reduction in data volume without imposing a significant loss of target parameter estimation sensitivity.

[3]Clutter cancellation has been ignored in this analysis for simplicity's sake. In subsequent sections, this stage is included. Incorporating clutter cancellation exacerbates the data processing issues and, as such, further supports the conclusions drawn in this section.

3.3. Clutter Cancellation via a Least-Squares Filter

From a target detection in noise perspective, the desirable surveillance signal (c.f. Eqn. 2) is $\boldsymbol{\eta_{s,n}}$. From a clutter-estimation and cancellation perspective, $\boldsymbol{\eta_{s,n}}$ is the 'noise' signal that we wish to retain. As such, with perfect knowledge of the transmitted waveform $x(t)$, we could calculate the optimal least-squares weight vector ($\boldsymbol{\omega_{opt}}$) by:

$$\boldsymbol{\omega_{opt,n}} = (X_C^H X_C)^{-1} X_C^H \boldsymbol{s_n} \tag{4}$$

In this perfect world, we may then use $\boldsymbol{\omega_{opt,n}}$ to estimate our (clutter free) desired signal (for each channel) by:

$$\overline{\boldsymbol{s_n}} = \boldsymbol{s_n} - (X_C \boldsymbol{\omega_{opt,n}}) \tag{5}$$

In practise, we don't know $\boldsymbol{x}$ (or its 2D form X_C) and must instead use $\boldsymbol{r}$ as an imperfect substitute. By using D as the representation of our imperfect knowledge, we can construct:

$$R = X_C + D \tag{6}$$

and substitute to achieve:

$$\begin{aligned}\boldsymbol{\omega_{sub,n}} &= (R^H R)^{-1} R^H \boldsymbol{s_n} \\ &= ((X_C^H X_C + X_C^H D + D^H X_C + D^H D)^{-1} \\ &\qquad (X_C^H \boldsymbol{s_n} + D^H \boldsymbol{s_n}) \\ &= \boldsymbol{\omega_{opt,n}} + \boldsymbol{e_n}\end{aligned} \tag{7}$$

As shown in Eqn. 7, the effect of the corruption (D) is to introduce an error to the 'optimal' weight vector estimate. When used to calculate our desired signal, we realise (the sub-optimal version of $\overline{\boldsymbol{s_n}}$):

$$\begin{aligned}\widetilde{\boldsymbol{s_n}} &= \boldsymbol{s_n} - ((X_C + D)\boldsymbol{\omega_{sub,n}}) \\ &= \boldsymbol{s_n} - X_C \boldsymbol{\omega_{opt,n}} + J\Phi_n\end{aligned} \tag{8}$$

where J is the $N_{CPI} \times C$ corruption due to our imperfect knowledge (common to all channels) and $\Phi_n = [e^{j\phi_{n,1}} \ldots e^{j\phi_{n,C}}]$ is a $C \times 1$ vector that contains the phase information corresponding to the distance between the antenna element and the clutter component being estimated and cancelled.

$$\widetilde{\boldsymbol{s_n}} = \overline{\boldsymbol{s_n}} + J\Phi_n = J\Phi_n + \boldsymbol{\eta_{s,n}} \tag{9}$$

In considering the formulation of the steering vectors of Eqn. 3 and the clutter cancelled signal of Eqn. 9, we can see a relationship between the phasor terms in both equations, as they are both generated by the same mechanism. As a result, in post delay-Doppler map direction finding, J will integrate constructively in the direction of the clutter component that dominates that delay cell. This indicates that J is not uniformly distributed in the spatial domain.

In the case of pre delay-Doppler map beamforming, the clutter components are scaled according to their direction of arrival and the beam's look direction. As J also depends on this scale term, this also results in a non-uniform distribution of the J term spatially.

4. RESULTS

Real-world multichannel data was collected using the DSTO-developed experimental passive radar system. The configuration of the experimental system deployed for data collection was the same as the scenario described in Section 3.1. The direction of the transmitter relative to the receiver was $164°$ relative to true north. Figure 4 shows the peak signal amplitude and azimuth of arrival maps that result from the application of the post-dDM direction finding scheme described earlier[4]. Figure 5 shows the histogram of the AoA information shown in Figure 4(b). These figures both show a clear bias toward the direction of arrival of the transmitter, indicating that there is structured signal across all delay-Doppler stemming from that direction. Whilst the clutter cancellation stage has reduced the direct path component by more than 50 dB, it is clear from the azimuth of arrival delay-Doppler map and histogram that there is still a dominant residual bias. Eqn. 9 indicates that this structured signal stems from the imperfect reference signal used to both calculate the direct path and clutter coefficients and to subsequently mitigate them. With perfect knowledge of the reference signal, it is expected that a uniform distribution of azimuth and elevation angles would result.

5. CONCLUSIONS

In passive radar, the reference signal is corrupted by both noise and multipath. As such, its use as a proxy for the originally transmitted signal will introduce imperfections into the processed signal. In this paper, we described a computationally efficient approach for multichannel processing that forms delay-Doppler maps on each element prior to DoA processing. Unfortunately, we also demonstrate both theoretically and with experimental results that the imperfections introduced in the clutter cancellation stage leads to a non-uniform distribution of noise energy in the spatial domain. Future work will seek to redress this deleterious effect.

[4]the elevation of arrival map has been excluded for brevity's sake

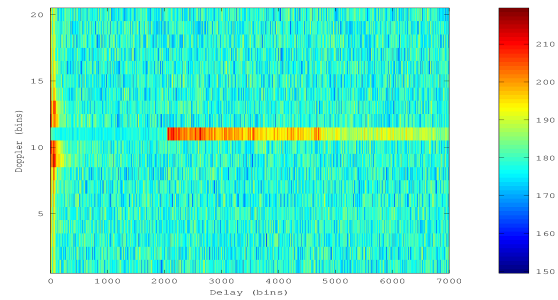

(a) Peak signal

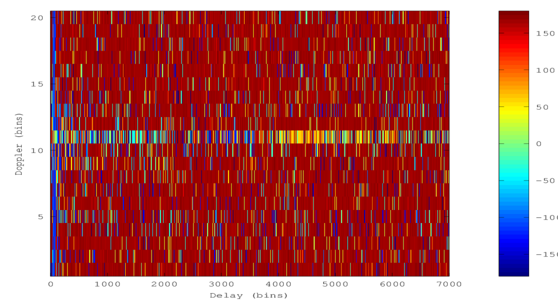

(b) Azimuth of Arrival

Fig. 4. DF on Clutter Cancelled signal

6. ACKNOWLEDGEMENTS

The author would like to thank Dr Lee Patton of Matrix Research for his intuition on the nature of the energy in the DPI direction, and the passive radar team at DSTO for their expertise and efforts in constructing the experimental system used to collect the data presented in this paper.

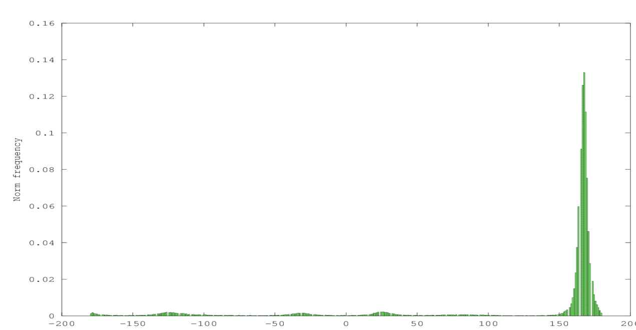

Fig. 5. Histogram of Azimuth of Arrival on Clutter Cancelled signal

7. REFERENCES

[1] R. Saini and M. Cherniakov, "DTV signal ambiguity function analysis for radar application," *IEE Proc. Radar Sonar Navig.*, vol. 152, no. 3, pp. 133–142, June 2005.

[2] D. Poullin, "Passive detection using digital broadcasters (DAB,DVB) with COFDM modulation," *IEE Proc. Radar Sonar Navig.*, vol. 152, no. 3, pp. 143–152, June 2005.

[3] J. Palmer, S. Palumbo, A. Summers, D. Merrett, and S. Howard, "DSTO's experimental geosynchronous satellite based PBR," in *Intl. Radar Conference*, Oct. 2009.

[4] J. Palmer, D. Merrett, S. Palumbo, J. Piyaratna, S. Capon, and H. Hansen, "Illuminator of opportunity bistatic radar research at DSTO," in *2008 Intl. Conf. on Radar*, Sept. 2008, pp. 701–705.

[5] W.C.Barott and B. Butka, "SABER–TDA: Passive coherent location of aircraft using XM–radio and a small ground station," in *2012 IEEE Radar Conference*, 2012, pp. 342–347.

[6] J.E. Palmer, H.A. Harms, S.J. Searle, and L.M. Davis, "DVB–T passive radar signal processing," *IEEE trans. on Signal Processing*, vol. 61, no. 8, pp. 2116–2126, 2013.

[7] M. Malanowski, K. Kulpa, and J. Misiurewicz, "Parade - passive radar demonstrator family development at warsaw university of technology," in *Microwaves, Radar and Remote Sensing Symposium, 2008. MRRS 2008*, Sept 2008, pp. 75–78.

[8] V. Winkler, M. Edrich, and A Schroder, "Transmitter identification and single frequency network characterization for the cassidian passive radar sensor," in *Radar Symposium (IRS), 2013 14th International*, June 2013, vol. 1, pp. 167–172.

[9] A Schroeder, M. Edrich, and V. Winkler, "Stationary cassidian fm passive radar demonstrator for 24/7 operation and sensor cluster measurements," in *Radar Symposium (IRS), 2013 14th International*, June 2013, vol. 1, pp. 161–166.

[10] C.I Coman, S. Gelsema, and C. Stolk, "Array antennas for passive covert radar applications," in *Antennas and Propagation (EuCAP), 2010 Proceedings of the Fourth European Conference on*, April 2010, pp. 1–4.

[11] H.A. Harms, L.M. Davis, and J.E. Palmer, "Understanding the signal structure in DVB–T signals for passive radar detection," in *IEEE Radar Conference*, May 2010, pp. 532–537.

[12] M. Radmard, F. Behnia, and M. Bastani, "Cross ambiguity function analysis of the '8k–mode' DVB–T for passive radar application," in *IEEE Radar Conference*, May 2010, pp. 242–246.